The Effect of Serrated Fins on the Flow Around a Circular Cylinder

Byong-Nam Ryu, Kyung-Chun Kim, Jung-Sook Boo*

School of Mechanical Engineering, Pusan National University,
30 Jangjeon-dong, Geumjeong-gu, Pusan 609-735, Korea

An experimental study is performed to investigate the characteristics of near wake flow behind a circular cylinder with serrated fins using a constant temperature anemometer and flow visualization. Various vortex shedding modes are observed. Fin height and pitch are closely related to the vortex shedding frequency after a certain transient Reynolds number. The through-velocity across the fins decreases with increasing fin height and decreasing fin pitch. Vortex shedding is affected strongly by the velocity distribution just on top of the finned tube. The weaker gradient of velocity distribution is shown as increasing the freestream velocity and the fin height, while decreasing the fin pitch. The weaker velocity gradient delays the entrainment flow and weakens its strength. As a result of this phenomenon, vortex shedding is decreased. The effective diameter is defined as a virtual circular cylinder diameter taking into account the volume of fins, while the hydraulic diameter is proposed to cover the effect of friction by the fin surfaces. The Strouhal number based upon the effective diameters seems to correlate well with that of a circular cylinder without fins. After a certain transient Reynolds number, the trend of the Strouhal number can be estimated by checking the ratio of effective diameter to inner diameter. The normalized velocity and turbulent intensity distributions with the hydraulic diameter exhibit the best correlation with the circular cylinder's data.

Key Words : Equivalent Diameter, Hydraulic Diameter, Effective Diameter, Vortex Formation Region, Vortex Shedding, Strouhal Number

Nomenclature

d_e : Effective Diameter
d_h : Hydraulic Diameter
d_i : Inner Diameter
d_o : Outer Diameter
f : Vortex Shedding Frequency
h : Fin Height
p : Fin Pitch
St : Strouhal Number $(St=fd/U_o)$
t : Fin Thickness
t_s : Exposure Time
U_{Max} : Streamwise Maximum Velocity
U_o : Freestream Velocity

X, Y : Rectangular Coordinate
$-$: Time Average

* Corresponding Author,
  E-mail : jsboo@pusan.ac.kr
  TEL : +82-51-510-2302; FAX : +82-51-512-9835
  School of Mechanical Engineering, Pusan National University, 30 Jangjeon-dong, Geumjeong-gu, Pusan 609-735, Korea. (Manuscript Received October 31, 2002; Revised March 26, 2003)

1. Introduction

Vortex shedding behind a bluff body is observed in a wide range of Reynolds numbers and in many industrial and environmental flows. Numerous studies on the mechanism of vortex formation have been carried out. Gerrard (1966) showed that the size of the vortex formation region is determined by the balance between the entrainment into the shear layer and the replenishing of fluid by induced reversed flow. As the Reynolds number is increased, the rate of entrainment will tend to increase. Hence, the vortex formation region must shrink in length. The end of the vortex formation region can be defined as the point at which the fluid from

outside of the wake crosses the center axis. Fluid is drawn across the wake by the action of the growing vortex on the other side. The end of the vortex formation region is also defined as that point of the maximum velocity fluctuation on the wake centerline with twice the vortex shedding frequency. Thereafter, Green and Gerrard (1993) insisted that the end of the vortex formation region corresponds with the point of maximum vorticity. This result has also been observed by Griffin (1995). The length of vortex formation is closely related to vortex shedding. If it is controlled by a body such as a split plate, the vortex shedding can be considerably modified (Gerrard, 1966; Apelt, 1973). Besides these studies, the effects of an electromagnetic force and a free surface on the flow behavior around a bluff body have been investigated by Kim and Lee (2002), and Lee and Daichin (2001).

The models used in this study are heat-exchanger tubes which are circular cylinders with serrated fins helically welded. Although the tubes are used to reduce the gas side heat resistance, not much information about flow characteristics is available in the literature. For engineers who design the optimal configuration of fin parameters, it is important to know the details to the flow fields around the serrated finned tube, such as fin height and fin pitch. The main purpose of this study is to scrutinize the flow characteristics around the serrated finned tube by focusing on the vortex shedding phenomenon. In the near wake behind the tube, ensemble and conditional measurements of velocity profiles are made in a wide range of Reynolds numbers. We suggest equivalent diameters which are used properly as the characteristic length scales because the tubes have spacing between the fins and the tube outer wall.

2. Experimental Apparatus and Procedure

To investigate the effect of serrated. fins on vortex shedding and its mechanism of the flow past cylinder, vortex shedding frequencies and velocity distributions are measured in a wind tunnel. A recirculating water tunnel is used for flow visualization. The wind tunnel is a closed circuit subsonic wind tunnel with a length of 36000 mm. The test section has dimensions of $2000(l) \times 700(h) \times 700(w)$ mm^3. The length of the contraction part is 1600 mm and the contraction ratio is 6.6 : 1. Free stream velocity, U_o, is controlled in a range of $0.5 \sim 60.0$ m/s, and its turbulent intensity is less than 0.2%. Uniformity of the velocity distribution in the test section excluding boundary layer is $1.0 \sim 1.5$ %. A constant temperature anemometer (TSI, IFA300), I-type (TSI, 1210-20), X-type (Kanomax, 0252R-T5) hot wire and split film probe (TSI, 1288) are used for velocity measurement. The X-type hot wire is used to find the vortex shedding frequency with the free stream velocity ranging from 5.0 to 30.0 m/s. The corresponding Reynolds number range based on the outer diameter of the tubes is 17000 to 185000. In this study, the X-axis is defined as the direction parallel to the freestream and the Y-axis is defined as the perpendicular direction with respect to both the X-axis and the cylinder axis. The velocity components along the X- and Y-axes and their turbulent intensities are designated as U, V and u_{rms}, v_{rms}, respectively. The position of the frequency measurement is $X/d_o=6.0$, $Y/d_o=0.0$ being the tube center. Calibration of the X-probe is carried out by the look-up table method. Hot wire signals are acquired with a sampling rate of 10 kHz (2 kHz for vortex shedding frequency measurement), and the number of each sample size is 40960 at every measuring point. For the reverse flow measurement in the near wake, a split film probe is set in the state of 90° rotation. This is the same method that was used by Kim and Jung (1991). The calibration method was proposed by Stock (1977, 1985).

The water tunnel used for flow visualization is driven by two impellers, and the total dimensions are about $12500(l) \times 5200(h) \times 2200(w)$ mm^3. The volume of water kept in the vertical circulating water tunnel is about 40 m^3. The test section dimensons are $5000(l) \times 1200(h) \times 1800(w)$ mm^3. The velocity in the test section is controlled from 0.1 to 2.0 m/s, and the velocity uniformity and

the turbulent intensity in the test section are 0.1% and 2.8%, respectively.

Polyvinyl chloride particles are used for flow visualization seeds. The specific gravity of the tracers is 1.02 and the diameter range is 100 to 200 μm. The light source is an Ar-Ion Laser (Coherent, Innova-70) the power of which is about 4 W. Particle images are recorded by a photographic still camera under the laser light sheet illumination. The configuration and geometry of the models used in this study are shown in Fig. 1. Details of the model geometry are summarized in Table 1. A total of 10 models are used including a bare tube for comparison. Four different outer diameters — 75, 85, 87, and 93 mm — and four different fin heights — 12, 17, 18, and 21 mm — are used in this research.

Table 1 Geometry of models

[mm]

Model	d_i	d_o	h	t	p	Remark
0	51	51	0	0	—	Circular Cylinder
1	51	75	12	1.0	8.45	
2	51	75	12	1.0	5.62	
3	51	85	17	1.0	6.76	
4	51	87	18	1.2	6.76	
5	51	87	18	1.2	5.62	
6	51	87	18	1.2	4.81	
7	51	87	18	1.2	4.05	
8	51	93	21	1.3	5.62	
9	51	93	21	1.3	4.05	
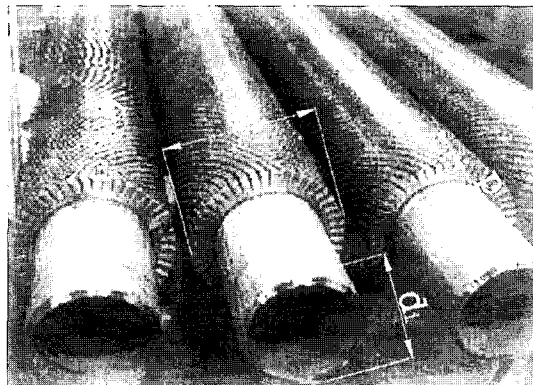
Fig. 1 Configuration of the model

3. Results and Discussion

The variation of the vortex shedding frequency versus the free stream velocities is shown in Fig. 2. As is the general tendency of a constant Strouhal number associated with a circular cylinder wake, the frequency increases linearly as freestream velocity increases in the present range. It is interesting to note that the vortex shedding frequency decreases as fin height increases and fin pitch decreases. For example, at the free stream velocity of 30 m/s, the frequency of Model #9 is about half of the bare tube. This is the effect of the fins, and is mainly due to the through-flow velocity crossing the fins. The through-flow velocity could be decreased with increasing fin height and decreasing fin pitch because of the increase in flow resistance by the fins. This factor may strongly affect the vortex shedding mechanism.

To clarify the effect of the fins, velocity distributions are acquired with various free stream velocities near the fin tubes using an I-type hot wire at $X/d_o=0.0$, $Y/d_o>0.5$. The results are demonstrated in Fig. 3. Velocity measurements inside the fins are possible at the position of the fins' middle height for Model #1 to #5, the fin spacings of which are wider than the others'. The measured through-flow velocity profiles are represented as in Fig. 3(b), (c). A rather surprising result is that the through velocity of Model #1 near the inner cylinder wall is much greater than that of the bare circular cylinder. It can be
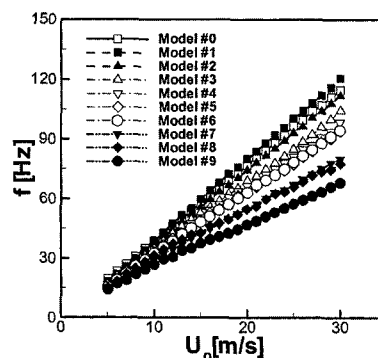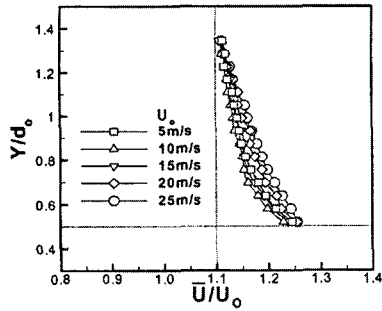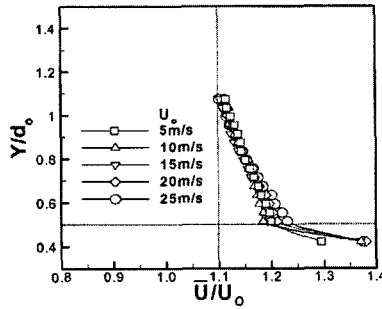

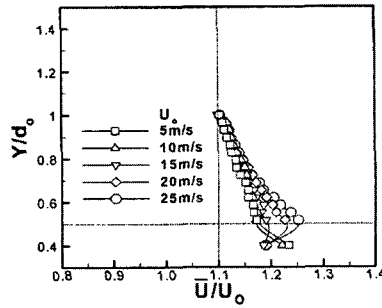**Fig. 2** Variation of vortex shedding frequency

explained that the through-flow may accelerate due to the narrowed passage resulting from the
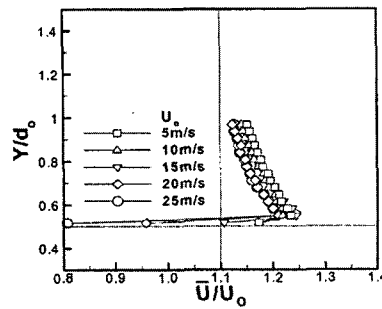

(a) Model #0

(b) Model #1

(c) Model #4

(d) Model #9

Fig. 3 Comparisons of the velocity distribution at $X/d_o=0.0$

thickness of fins. In Fig. 3(c) Model #4, the velocity of the middle part of the fin height decreases as the freestream velocity increases due to flow resistence, and the position of maximum velocity moves in the Y-direction. To compare the velocities near the inner cylinder, the velocity of the circular cylinder and of Model #1, they were 1.25 and 1.29 to 1.38 times the freestream velocity, respectively. But in case Model #4, the velocity decreases only marginally.

According to Chang's results (1979), the maximum velocity near a circular cylinder accelerates by approximately 1.6 U_o. Chang (1979) argued that the velocity near the wall reaches its maximum near 80° position then the velocity decreases as the flow moves to the downstream. Therefore, the present values (1.25 Uo in the case of the circular cylinder ; 1.29 to 1.38 U_o in the case of Model #1) are acceptable because the angle of the measuring point in this study is 90° from the stagnation point. It seems that the separation is delayed because increased turbulent intensity caused by the fins promotes momentum transfer from the freestream. Therefore, the maximum velocity of the fin tubes in Model #1 is greater than the circular cylinder's value, and this is observed in Models #2 and #3, too. When fin height increases and pitch decreases, the turbulent intensity increases, and the friction force of fluid which flows between fins also increases. This causes the boundary layer to be developed. This development of boundary layer makes the velocity gradient between the inner cylinder and the position of maximum velocity decrease and affects vortex shedding.

In Fig. 3(d), Model #9 shows the opposite tendencies since the fin spacing is too narrow to pass through easily; hence the velocity decreases and the position of maximum velocity moves away from the cylinder wall. The effect of the Reynolds number is also shown in the velocity gradient. One can expect that the velocity profile near the separation point attributes to the kinematics of vortex shedding.

Velocity distributions are classified according to three modes as shown in Fig. 4. Friction can be increased by increasing fin height and free stream

velocity and by decreasing fin pitch. With increasing flow friction, the velocity distributions of the through flows are varied from type "A" to "C" as indicated in Fig. 4. Type "C" has the lowest velocity gradient in the region between the cylinder and the fin. It makes for a much weaker shear layer before flow separation, so that the length of the recirculating zone becomes longer.

Usually, the weaker shear layer causes a reduction of vortex shedding frequency. Similar results have also been observed by Gerrard et al.(1966, 1993). They introduced the relationship between the size of the formation region, the strength of vortices and the frequency of vortex shedding. According to their conclusions, the higher velocity gradient observed in Model #1 compared with the circular cylinder (Model #0) makes the entrainment flow much stronger and is followed by an increase of vortex shedding frequency. But, too many fins change the velocity profiles from type "A" to type "B" or "C", so that the entrainment flow moves downstream and is weakened. As a result, the vortex shedding frequency decreases.

Flow visualization results in the water channel are represented in Fig. 5. In this case, the water flow velocity is 0.99 m/s, which corresponds to 15.0 m/s in the wind tunnel by dynamic similarity. The exposure time of the still camera is 0.25 of a second. Because of the high through velocity, Model #1 shows a shorter formation region compared with the bare tube case, Model #0 (see Fig. 5(a) and (b)). This result confirms our explanation about the effect of fins on the vortex
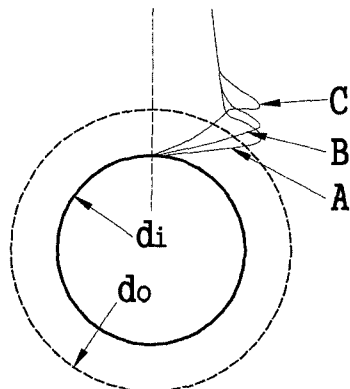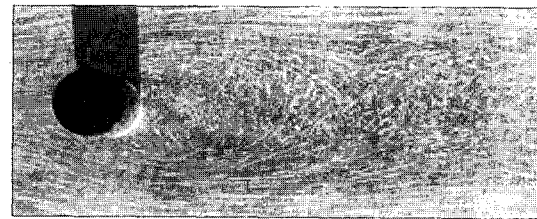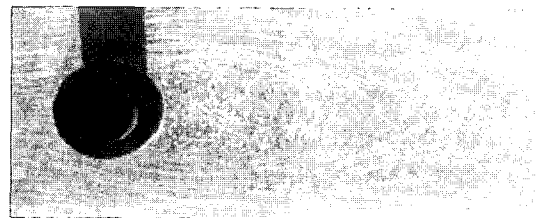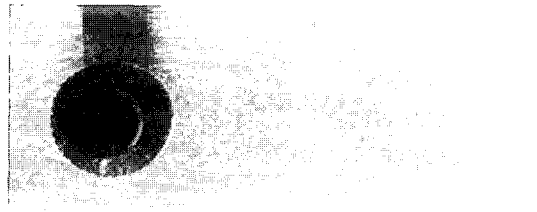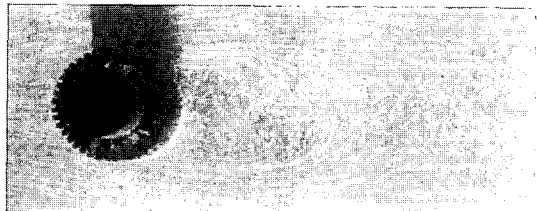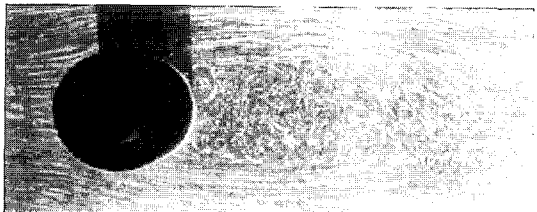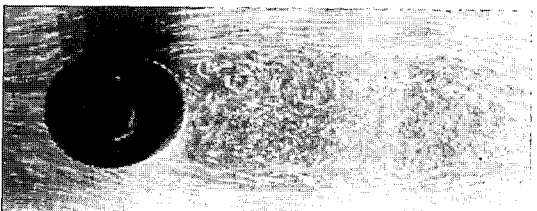

(a) Model #0

(b) Model #1

(c) Model #3

(d) Model #5

(e) Model #8

(f) Model #9

Fig. 5 Results of flow visualization of various models(U_o=0.99 m/s, t_s=1/4 sec)

Fig. 4 Sketch of the velocity distribution

shedding mechanism. The width of wakes in the Y-direction of the fin tubes become wider as fin pitch decrease because of the retarding velocity on the fin tube and the growing boundary layers. In Figs. 5(e) and (f), it is hard to find any closed formation region within the field of view.

For measuring the vortex formation length, the U-component velocity is determined using a split film probe at $0.8 \leq X/d_o \leq 2.6$, $-1.0 \leq Y/d_o \leq 0.2$. This result is used to plot the equi-velocity contours. For entire models, the vortex formation length is obtained by the method that a position crossing the $\overline{U}/U_o = 0.0$ contour line and the $Y/d_o = 0.0$ line is determined to be at the end of the vortex formation region. These results are plotted in Fig. 6. In Fig. 6(a), where the vortex formation length, L_B is normalized by the outer diameter, d_o, the vortex formation length of Models #3 to #6 are less than those of Models #0 to #2. Comparison of the vortex formation length as normalized by the inner diameter is necessary, because the position of the entrainment flow ex-

pected in Fig. 4 is considered as being normalized by the inner cylinder diameter.

In Fig. 6(b) the vortex formation length, normalized by the inner diameter, d_i, increases approximately as fin density increases, as was seen in the flow visualization results. As freestream velocity increases from 5.0 m/s to 10.0 m/s, the vortex formation lengths of all the models are reduced. But, with increasing freestream velocity, three different trends are represented, which are increasing, decreasing and constant trend of vortex formation length.

In the case of Models #1 and #2, as freestream velocity increases, the vortex formation lengths are slightly reduced. But, in the case of Models #7 to #9, the lengths increase, and in the case of Models #3 to #6, the length are nearly constant with increasing freestream velocity.

As mentioned above, the finned tube has spaces between the fins. In order to compare the Strouhal numbers obtained by the serrated finned tube with those of the normal circular cylinder, it is necessary to choose a proper length scale for the finned tube. Many different choices of tube diameters are available. In Fig. 7, the fixed geometrical diameters are the inner diameter d_i and the outer diameter d_o. However, we need an equivalent diameter taking into account the fins. Therefore, we define a hydraulic diameter, d_h and an effective diameter, d_e, as follows :

Hydraulic diameter, d_h : A diameter which takes into account the passage between fins ;

$$d_h = d_o - 2 \times \left(\frac{4 \times (p-t) \times h}{p-t+2 \times h} \right) \qquad (1)$$
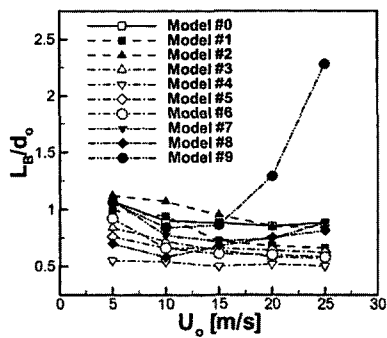
(a) Normalization by d_o
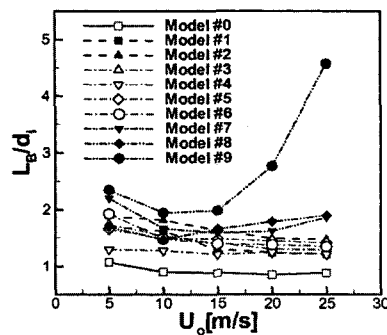
(b) Normalization by d_i

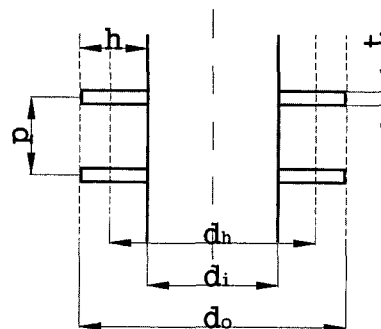**Fig. 6** Vortex formation length of various models

Fig. 7 Concept of hydraulic diameter

Table 2 Equivalent diameters

[mm]

Model	d_e	d_h	Model	d_e	d_h
0	Cylinder		5	60.3	71.3
1	54.2	52.2	6	61.8	73.9
2	55.8	59.5	7	63.6	76.4
3	57.1	65.3	8	63.1	77.3
4	58.8	67.7	9	67.2	82.7

Effective diameter, d_e : A diameter of the circular cylinder which has a volume equal to that of the fin tube.
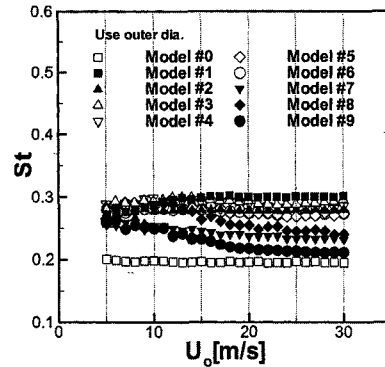
The values of hydraulic diameters and equivalent diameters are shown in Table 2. The d_h and d_e have dimensions of 69.6—88.9% and 67.2—74.4% of do, respectively.

Strouhal numbers measured by hot wire at the near wakes of various models are normalized by the defined equivalent and outer diameters as shown in Fig. 8. The values of Strouhal number normalized by the outer diameters are much higher than those of the circular cylinder. This result indicates that the outer diameter is not a more adequate length parameter since it does not reflect any effect of the fins. However, equivalent diameters seem to be reasonable scales. Especially, the effective diameter works well to fit all the data with that of the bare tube at the lowest Reynolds number.

If we carefully look at Fig. 8(b), there are three different trends of Strouhal number with respect to Reynolds number as follows :

(1) The Strouhal number is constant (like a circular cylinder's data) in the range of Reynolds number (Models #3 to #6);

(2) The Strouhal number increases ·in the Reynolds number and then saturates (Models #1 to #2);

(3) The Strouhal number decreases after a certain transition region (Models #7 to #9).
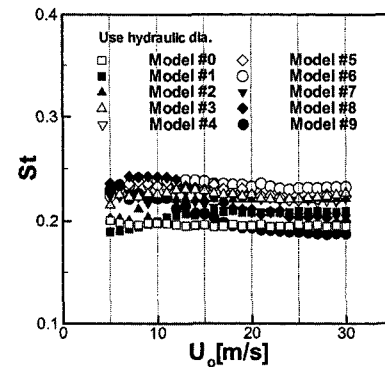
The results are very interesting and imply that the effect of fins on vortex shedding is vivid. Furthermore, fins may increase vortex frequency for a certain geometrical parameter, and vice versa. The differences in the through-flow velo-
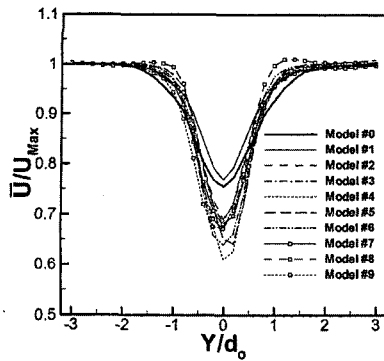

(a) Outer diameter, d_o
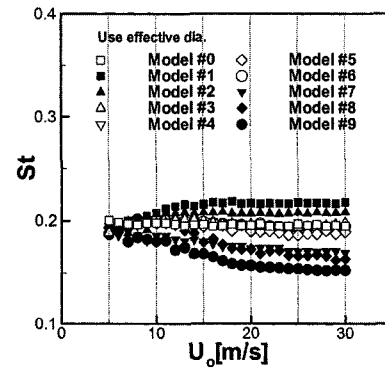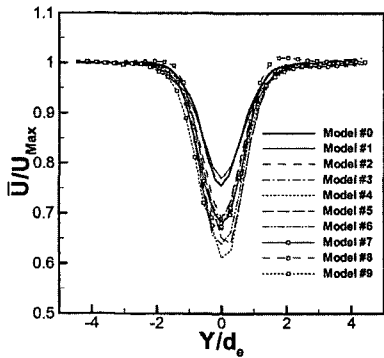

(b) Effective diameter, d_e

(c) Hydraulic diameter, d_h

Fig. 8 Strouhal numbers of various models with outer and equivalent diameters

city profiles confirm, as suggested in Fig. 4, that there exist different vortex shedding mechanisms with different geometrical arrangements. It can be explained that Models #1 and #2 accelerate the fluid velocity at the area between two adjacent fins and the strong shear layer produces a faster roll-up process. With slight increase in fin density, acceleration may diminish due to the increase
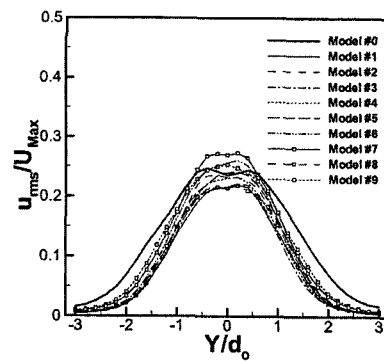
(a) Outer diameter, d_o
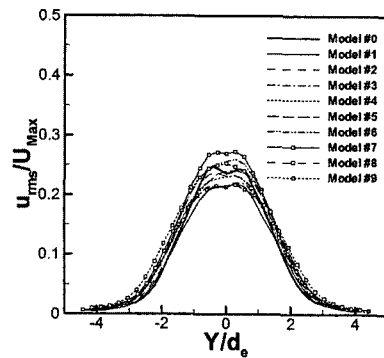

(b) Effective diameter, d_e
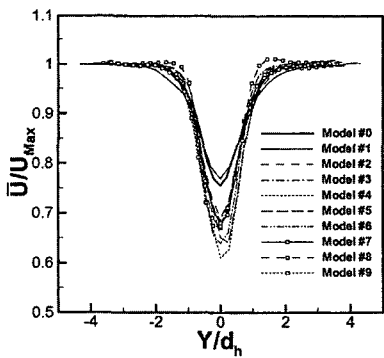
(c) Hydraulic diameter, d_h

Fig. 9 Comparisons of the time mean velocity with various diameters at $X/d_o=5.0$, $U_o=10.0$ m/s

(a) Outer diameter, d_o

(b) Effective diameter, d_e

(c) Hydraulic diameter, d_h

Fig. 10 Comparisons of the streamwise turbulent intensity with various diameters at $X/d_o=5.0$, $U_o=10.0$ m/s
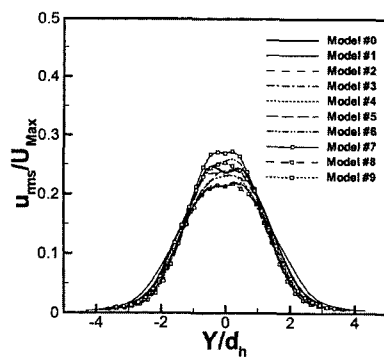
in wall friction, hence the velocity gradient near the finned tube turns out to be almost equal to that of the circular cylinder. Consequently, the vortex shedding mechanism might be the same as with the circular cylinders, which keeps the Strouhal number constant with a certain range of Reynolds number (see Models #3 to #5). With a further increase in fin density, the through flow faces a strong adverse pressure gradient since the

gap between two adjacent fins is too narrow. This configuration (Models #7 to #9) causes a relatively weak velocity gradient near the separation point, and then a decreasing Strouhal number with increasing wake width.

Once the effective diameter can be used for scaling the Strouhal number properly for the serrated finned tube wake, the usefulness should
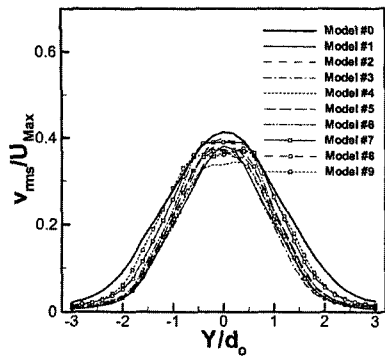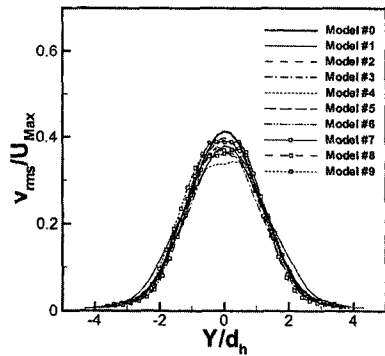
(a) Outer diameter, d_o
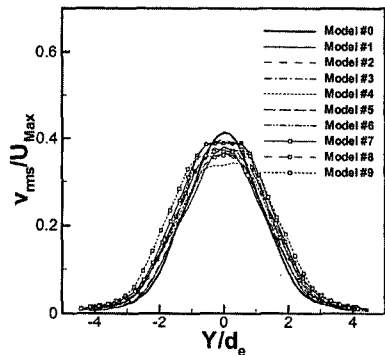
(b) Effective diameter, d_e

(c) Hydraulic diameter, d_h

Fig. 11 Comparisons of the lateral turbulent intensity with various diameters at $X/d_o=5.0$, $U_o=10.0$ m/s

be checked for both mean velocity profile and turbulent intensity distributions in the wake. Fig. 9 depicts the normalized mean velocity profiles taken at $X/d_o=5.0$ by various diameters. In general, the velocity defect becomes stronger with increasing fin height and decreasing fin pitch mainly because of the increase in friction. Of course, the difference comes from the differences

in vortex formation length. As can be seen in Fig. 9(a), the velocity profile normalized by the outer diameter shows many scatters compared with other equivalent diameters which take into account the effect of the fins. The best correlation with the data of a circular cylinder is made when the hydraulic diameter is used as the length scale. It can be explained that the hydraulic diameter reflects friction forces due to the fins.

The distributions of streamwise and lateral turbulent intensity measured at $X/d_o=5.0$ are demonstrated in Fig. 10 and Fig. 11. Again, three different diameters are used for scaling. It is interesting to note that the intensity profiles obtained in the wakes of the finned tube seem to be nearly the same as those obtained in the case of the bare tube wake. There are many scatters when the outer diameter is used for normalization. Due to the gap between the fins, the half width of the turbulent intensity profiles get narrow compared with the circular cylinder case as shown in Fig. 10(a) and Fig. 11(a). The best correlation is accomplished by using the hydraulic diameter as the characteristic length. A slight lack of correlation is shown in the maximum intensity region, but the correlation of the half width looks excellent.

4. Conclusions

The characteristics of vortex shedding and near wake of the circular cylinder with serrated fins were investigated experimentally for various free stream velocities. The following conclusions were obtained.

(1) Three different modes of Strouhal number versus Reynolds number were firstly observed in the wakes behind serrated finned tube cylinders. In general, sparse fins increase the Strouhal number with increasing Reynolds number, while dense fins decrease the Strouhal number with increasing Reynolds number.

(2) Three different categories of velocity profiles inside the gap between the fins were observed. These phenomena are attributable to the three different modes of Strouhal number behavior.

(3) The lower velocity gradient is in the

through flow, the longer the length of vortex formation. The weak shear layer moves the entrainment flow further downstream and decreases the vortex shedding frequency.

(4) The effective diameter and hydraulic diameter are proposed for taking into account the effect of the fins.

(5) The Strouhal number based on the effective diameter correlates well with that of the circular cylinder. The mean velocity and turbulent intensity distributions are well correlated with the hydraulic diameters.

References

Apelt, C. J., West, G. S. and Szewczyk, A. A., 1973, "The Effects of Wake Splitter Plates on the Flow Past a Circular Cylinder in the Range $10^4 < R < 5 \times 10^4$," *J. Fluid Mech.*, Vol. 61, Part 1, pp. 187~198.

Chang, Paul K., 1979, *Separation of Flow*, Pochinchai Printing Co., Ltd., Korea, pp. 11~18.

Gerrard, J. H., 1966, "The Mechanics of the Formation Region of Vortices behind Bluff Bodies," *J. Fluid Mech.* Vol. 25, Part 2, pp. 401~413.

Green, R. B. and Gerrard, J. H., 1993, "Vorticity Measurements in the Near Wake of a Circular Cylinder at Low Reynolds Numbers," *J.*

Fluid Mech. Vol. 246, pp. 675~691.

Griffin, Owen M., 1995, "A Note on Bluff Body Vortex Formation," *J. Fluid Mech.*, Vol. 284, pp. 217~224.

Kim, K. C. and Jung, Y. B., 1991, "The Effect of Free Stream Turbulence of the Near Wake behind a Circular Cylinder," *Transactions of the KSME*, Vol. 15, No. 6, pp. 2062~2072.

Kim, S. J. and Lee, C. M., 2002, "Numerical Investigation of Cross-Flow Around a Circular Cylinder at a Low-Reynolds Number Flow Under an Electromagnetic Force," *KSME International Journal*, Vol. 16, No. 3, pp. 363~375

Lee, S. J. and Daichin, 2001, "Flow Structure of the Wake behind an Elliptic Cylinder Close to a Free Surface," *KSME International Journal*, Vol. 15, No. 12, pp. 1784~1793.

Stock, David E. and Jaballa, Tuhami M., 1985, "Turbulence Measurements Using Split-Film Anemometry," *Proc. Int. Symp. on Refined Flow Modeling and Turbulence Measurement* (University of Iowa), H15-1-10.

Stock, D. E., Wells, M. R., Barriga, A. and Crowe, C. T., 1977, "Application of Split-Film Anemometry to Low-Speed with High Turbulence Intensity and Recirculation as Found in Electrostatic Precipitators," *Proc. Fifth Biennial Symp. on Turbulence* (University of Missouri, Rolla), pp. 117-123.